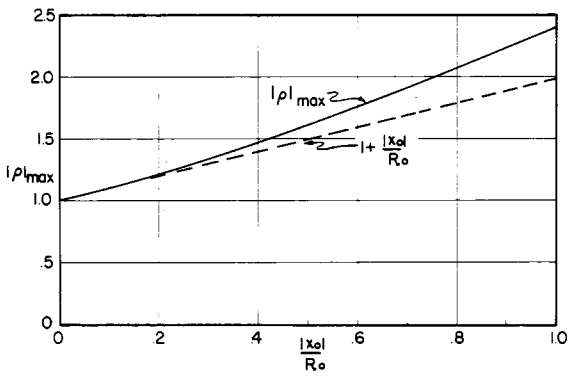

Fig. 1. Maximum obtainable value of $|\rho|$ vs. $|X_0|/R_0$.

The value of $|\rho|_{\max_{R_L,X_L}}$ is plotted in Fig. 1 as a function of $|X_0|/R_0$. This graph then gives the maximum obtainable value of $|\rho|$ for a transmission line in terms of $|X_0|/R_0$. Note that since R_0 must be greater than $|X_0|$, the largest value of $|\rho|$ obtainable on a physically realizable passive line with a passive load is 2.414. For the case where $|X_0| \ll R_0$, the following expression is seen to give a good approximation to $|\rho|_{\max_{R_L,X_L}}$:

$$|\rho|_{\max_{R_L,X_L}} \approx 1 + \frac{|X_0|}{R_0}. \tag{17}$$

Even though $|\rho|$ may be greater than unity the sign of the time-averaged power dissipated in the load $P_L = \frac{1}{2}\,\mathrm{Re}\, V_L I_L^*$ must be non-negative for a passive load. From (1) through (10) it may be shown that

$$P_L = \frac{1}{2}\mathrm{Re}\left[(V_1 + V_2)\frac{(V_1^* - V_2^*)}{Z_0^*}\right] = \frac{1}{2}\left|\frac{V_1}{Z_0}\right|^2 R_0\left[1 - |\rho|^2 - 2\frac{X_0}{R_0}\,\mathrm{Im}\,\rho\right]. \tag{18}$$

Since neither P_L nor R_0 can be negative it can be seen from (18) that the following condition must hold for a passive load

$$\left[1 - |\rho|^2 - 2\frac{X_0}{R_0}\,\mathrm{Im}\,\rho\right] \geq 0. \tag{19}$$

But using (10) it is found that

$$\left[1 - |\rho|^2 - 2\frac{X_0}{R_0}\,\mathrm{Im}\,\rho\right] = \frac{4R_L}{DR_0}(R_0^2 + X_0^2). \tag{20}$$

Thus, since a passive load implies that $R_L \geq 0$, it follows from (11) and (20) that $|\rho|^2$ as given by (9) does indeed satisfy the passivity criterion (19).

The condition $|\rho| > 1$ is sometimes misinterpreted to indicate that the magnitude of the reflected power is greater than the incident power. The error in this argument is that for a nondistortionless transmission line (for which $|\rho|$ may be greater than unity) the concept of incident and reflected powers is not in general valid. The time-average power $P(s)$, at any point s on the transmission line, associated with the voltage and the current as given by (1) may, with the help of (2) and (7), be shown to be

$$P(s) = \tfrac{1}{2}\,\mathrm{Re}\, V(s)I^*(s) = P_i + P_r + P_c \tag{21}$$

where

$$P_i = \frac{1}{2}\left|\frac{V_1}{Z_0}\right|^2 R_0 e^{2\alpha s}, \tag{22}$$

$$P_r = -\frac{1}{2}\left|\frac{V_2}{Z_0}\right|^2 R_0 e^{-2\alpha s} = -P_i|\rho|^2 e^{-4\alpha s}, \tag{23}$$

$$P_c = -X_0\,\mathrm{Im}\left[\frac{V_2}{Z_0}\frac{V_1^*}{Z_0^*}e^{-2j\beta s}\right] = -X_0\left|\frac{V_1}{Z_0}\right|^2 |\rho|\sin(\theta_\rho - 2\beta s). \tag{24}$$

Consider the terms $V_1 e^{\gamma s}$ and $(V_1/Z_0)e^{\gamma s}$ in (1). By replacing γ by $\alpha + j\beta$ and including the time factor, it may easily be verified that these terms correspond to voltage and current distributions along the line for which the phase of oscillation moves with uniform velocity ω/β in the negative s direction. It is therefore common to interpret these terms, respectively, as voltage and current waves travelling in the negative s direction, or simply as "incident" waves. The time-average power associated with the incident waves, if they exist alone on the line, is P_i as given in (22). Similarly the terms $V_2 e^{-\gamma s}$ and $-(V_2/Z_0)e^{-\gamma s}$ are identified as waves progressing in the positive s direction or simply as "reflected" waves. The power associated with these waves, if they exist alone, is P_r as given in (23). When both incident and reflected waves exist on a nondistortionless line simultaneously, the total voltage (current) at a point s on the line is a linear superposition of the incident and reflected voltage (current) waves at that point as given by (1). However, the net power flow in the negative s direction is not in general the sum of the incident and reflected power[3] as may be seen from (21), but carries an additional term P_c. Observe that P_c is positive at some points and negative at others. It is seen from (24) that for $X_0 = 0$ (a distortionless or lossless line) $P_c = 0$ for all s and then it is correct to separate the total power $P(s)$ associated with $V(s)$ and $I(s)$ into the sum of the incident and the reflected powers. Thus for lossless or distortionless lines corresponding to $X_0 = 0$, $|\rho|$ is always less than unity and the magnitude of the reflected power is seen to be always less than the incident power, which is in accordance with what should obtain for a passive load.

In conclusion, it is shown that the fact that the magnitude of the voltage reflection coefficient is greater than unity does not necessarily imply an active load and that in situations where it is physically meaningful to separate the total power into the sum of the incident and the reflected powers, it is evident that the magnitude of the reflected power is less than the incident power, as it should be for a passive load.

R. J. Vernon
S. R. Seshadri
Dept. of Elec. Engrg.
University of Wisconsin
Madison, Wis. 53706

[3] Note that the reflected power carries a minus sign with it indicating its direction of flow.

Comment on "Measurement of Delayed Time Differences on the Photocathode Surface of a Photomultiplier"

***Abstract*—The relative response time delay at different surface points on the photocathode of a photomultiplier tube was measured by determining the relative modulation phase shift of modulated light. The measurements were made on a different type of photomultiplier tube than previously reported measurements, and results were very dissimilar.**

In the above letter[1] Suematsu, Normura, and Tomita recently described a method for measuring the response time delay versus the position of the activated portion of the photocathode of a photomultiplier tube. They also give experimental results of response time dispersion for an RCA 7102 photomultiplier tube. We have mapped the relative time delay versus photocathode position for an RCA 7265 photomultiplier and obtained very dissimilar results. Our method involved modulating a 6328 Å laser beam with a 25 MHz sinusoid and directing the beam onto a 1 mm aperture after attenuating it to suitable levels. The photomultiplier tube was then mechanically scanned behind the aperture, and the relative phase of the detected modulation was recorded. The data was then plotted as a set of equal time delay contours on a plane representing the photocathode surface.

The topography of the time delay surface for the 7265 tube is not nearly so simple as the regularly spaced and nearly circular contours obtained for the 7102 tube by Suematsu *et al.* For our 7265, we found that the minimum transit time occurred anomalously for a small area well removed from the center of the photocathode area. Aside from this anomalous region, the

Manuscript received September 27, 1968. This research was supported in part by NASA Grant 37-003-026.

[1] Y. Suematsu, K. Normura, and E. Tomita, *Proc. IEEE (Letters)*, vol. 56, pp. 1405–1406, August 1968.

remainder of the time delay surface is best described as gently undulating in irregular fashion. Choosing the minimum transit time as the reference value, the relative transit times outside the small anomalous region varied between extremes of 0.9 ns and 1.7 ns for a photocathode area about 2 cm in diameter. The transit time variation over the central region 1 cm in diameter (which does not include the anomalous region) is about 0.6 ns.

The data reported here were taken with the tube operated at the relatively low potential of 1000 V. Operation at high potentials does not change the appearance of the time delay surface but does effect a slight reduction in the amount of variation.

W. L. KURIGER
J. L. BOWIE
Y. K. LEE
Dept. of Elec. Engrg.
University of Oklahoma
Norman, Okla. 73069

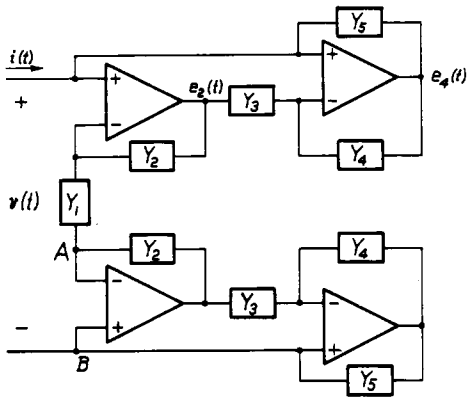

Fig. 1. A circuit for simulating voltage-current relations. In applications where one input terminal is to be grounded, nodes A and B can be grounded.

A Method for Realizing Time-Varying Circuit Elements

***Abstract*—A practical method is presented for realizing time-varying circuit components whose instantaneous element values depend on externally generated digital control signals. These signals control the value of a discrete-state resistor in an operational amplifier circuit. The method was used to realize linear time-varying inductors and capacitors which were built and tested.**

This letter describes a method for realizing time-varying circuit components whose instantaneous element values depend on externally generated digital control signals. These digital signals control the value of a discrete-state resistor in an operational amplifier circuit. The ideas involved will be illustrated by showing how we used the circuits in Fig. 1 to simulate linear time-varying inductors and capacitors.[1]

In Fig. 1 the admittance operators Y_1, Y_2, Y_3, Y_4, and Y_5 are not restricted to being linear; however, the inverse operations Y_1^{-1}, $(Y_5Y_3)^{-1}$, and Y_5^{-1} are assumed to be well defined. If the gains of all the differential amplifiers are large in comparison with unity, and if nodes A and B in Fig. 1 are grounded, then $Y_1(v)=Y_2(v-e_2)$, $Y_3(v-e_2)=Y_4(v-e_4)$, and $i=Y_5(v-e_4)$. It follows that

$$v = Y_1^{-1}(Y_2([Y_5Y_3]^{-1}(Y_5(Y_4(Y_5^{-1}(i)))))). \tag{1}$$

Equation (1) also applies if the circuit is used in its ungrounded configuration. The circuit in Fig. 1 will simulate a variety of interesting v-i relations, which will be nonlinear if nonlinear two-terminal elements are available.

If $Y_1=G_1(t)\cdot$, $Y_2=G_2\cdot$, and $Y_3=G_3\cdot$, $Y_4=G_4\cdot$, and $Y_5=C_5(d/dt)\cdot$, then $i(t)=d(Cv)/dt$, where $C(t)=G_3C_5G_1(t)/G_2G_4$. Alternately, if $Y_1=G_1\cdot$, $Y_2=C_2(d(dt)\cdot$, $Y_3=G_3(t)\cdot$, $Y_4=G_4\cdot$, and $Y_5=G_5\cdot$, then $v=d(Li)/dt$, where $L(t)=G_4C_2/G_1G_5G_3(t)$. It follows that time-varying inductors and capacitors can be realized if time-varying conductors are available.

Fig. 2(a) shows a conductance of value $G=gB$, where

$$B = \sum_{k=0}^{n-1} b_k 2^k.$$

Binary digit $b_k=0$ if the kth switch is open; $b_k=1$ if the kth switch is closed. The digital interpolating system, which enables conductance $G(t)$ to approximate in stepwise fashion an arbitrary time function [see Fig. 2(b)], operates as follows. The values of $B(t)$ at times $\cdots$, T_{i-1}, T_i, T_{i+1}, $\cdots$ are stored in a digital computer or other digital storage device. At time T_{i-1}, the n-bit approximation of $B(T_i)$ is transferred from the computer to the lower side of the digital comparator. At the same time, an additional m bits specifies the period of the clock pulse generator during the time interval

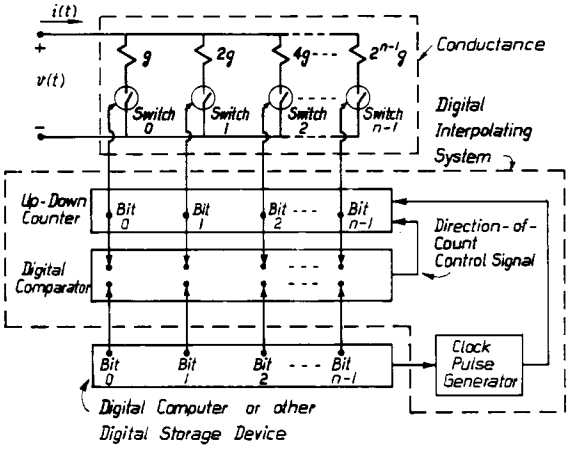

Fig. 2. (a) A discrete-state time-varying conductance and its control circuitry. (b) Stepwise approximation to a continuous time function. All steps are of equal height.

$T_{i-1} \leq t < T_i$. This pulse generator controls the rate at which the up-down counter increments. The binary number

$$\sum_{k=0}^{n-1} b_k 2^k$$

from the counter controls the positions of the n switches in Fig. 2(a), and also goes to the upper side of the digital comparator. If the number from the counter exceeds $B(T_i)$ from the computer, the comparator instructs the counter to count down one increment; if the counter's number is less than $B(T_i)$, the counter counts up one increment. The counter stops incrementing when its number equals $B(T_i)$. Correct adjustment of the clock pulse generator at $t=T_{i-1}$ enables the number in the counter to reach the desired value at $t=T_i$. The difference between a continuous $B(t)$ and its stepwise approximation can always be decreased by increasing the number of bits n and by decreasing the time intervals T_i-T_{i-1}.

Fig. 3(a) shows an actual circuit which was used to simulate an ungrounded time-varying inductor in a situation where $|idL/dt| \ll |Ldi/dt|$.

Manuscript received September 9, 1968. This work was supported by the National Research Council of Canada under Grant NRC A-3308.

[1] The circuit in Fig. 1 was used by Riordan[2] to simulate steady-state impedance functions.

[2] R. H. S. Riordan, "Simulated inductors using differential amplifiers," *Electronics Lett.*, vol. 3, pp. 50–51, February 1967.